

Image Fusion Using Optimization of Statistical Measurements

Laurent Oudre Tania Stathaki and Nikolaos Mitianoudis

Imperial College London

Abstract

The purpose of image fusion is to create a perceptually enhanced image from a set of multi-focus or multi-sensors images. In the methods we are about to describe we do not *a priori* know the ground truth image: these are blind fusion methods. There are mainly two groups of fusion methods depending on the signal domain they are applied: spatial domain methods and transform domain methods. The Dispersion Minimisation Fusion (DMF) and Kurtosis Maximisation Fusion (KMF) based techniques we are going to discuss are spatial domain methods that is to say the fusion is simply performed on the image itself. In this work we propose to linearly combine the input images with appropriate weights estimated using specific mathematical performance criteria which evaluate in various ways improvement in visual perception. More specifically, in order to estimate the weights we propose iterative methods which use cost functions based on two statistical parameters, i.e., the dispersion and the kurtosis. The optimisation of the proposed cost functions enables us to obtain a fused image which is less distorted compared to the input ones.

1. Introduction

Let us have K source images X_1, \dots, X_K describing different realizations of the same true scene F . The available images have been acquired from different sensors (multi-sensor scenario) or they are of the same type but exhibit different types of distortion, as for example blurring (multi-focus scenario). Our aim is to create from these images a single image Y which will be perceptually enhanced. The composite image should contain a more useful description of the scene than the one provided by any of the individual sources, and therefore, should be more useful for human visual or machine perception. The task of combining images to form a single improved image is called *image fusion*. Image fusion has been used in many fields such as aerial and satellite imaging, medical imaging, robot vision etc. In recent years image fusion has become an important and useful technique for image analysis, computer vision, concealed weapon detection, autonomous landing guidance and others. Image fusion can be performed either in the spatial or in the transform domain.

As far as the transform domain fusion methods are concerned the input images are first transformed into a new domain, then fused and the result is converted back by an inverse transform. Popular transform domain fusion methods are for example the Dual-Tree Wavelet Transform (DT-WT)

method [7] or the Independent Component Analysis (ICA) method [4]. In these methods the fusion coefficients are calculated with either pixel based or region based fusion rules.

The methods we are proposing in this work are spatial domain methods, that is to say, we work on the input images directly. A linear combination of the available source images is used, where the weights are estimated using novel optimisation formulations.

In order to understand the mechanisms behind the proposed fusion rules a thorough mathematical background and some notations are required. Section 2 of this chapter will be dedicated to the notations, the definitions and the problem formulation. Sections 3 and 4 are dedicated to the description of the proposed methods, as well as modified versions of them. The first method we propose is the Distortion Minimization Fusion (DMF). This spatial domain fusion technique utilizes the cost function of one of the most studied and implemented methods, i.e., the Constant Modulus (CM) algorithm, and the concept of signal dispersion [8]. An iterative process updates at every step the weights for the pixels by minimizing a function of the dispersion of the unknown original image. An alternative technique is also proposed where we use the Central Limit Theorem and the characteristics of smoothing (blurring) operators to assume that the non-Gaussianity is an indicator of image quality. The statistical parameter we consider to measure non-Gaussianity is the absolute value of kurtosis. This method is called Kurtosis Maximization Fusion (KMF). The additional methods we shall introduce are improvements of the previous ones. Section 5 is a presentation of indicative results we obtain with the proposed methods.

2. Mathematical Preliminaries

Assume K two dimensional source digital images X_1, \dots, X_K of equal size $M \times N$ describing the same true scene F . The images are registered to each other. By scanning the rows sequentially we transfer each image X_k to a vector \underline{x}_k (lexicographic ordering) with elements $x_k(n)$ where $n \in [1, MN]$. The aim of image fusion is to reconstruct a fused image Y which demonstrates an improved image quality over any individual image X_k . For the fused image we also use its lexicographically ordered version \underline{y} with elements $y(n)$.

To examine a spatially adaptive image fusion scheme we are interested in assigning to the n^{th} pixel $x_k(n)$ a distinct weight $w_k(n)$ that measures the contribution of the pixel $x_k(n)$ to the fused pixel $y(n)$. It is convenient to gather all the weights and intensity values at the n^{th} pixel location together and denote them by single vectors as follows

$$\underline{w}(n) = [w_1(n), \dots, w_K(n)]^T \quad (1)$$

and

$$\underline{x}(n) = [x_1(n), \dots, x_K(n)]^T \quad (2)$$

where $n \in [1, MN]$.

Consequently the n^{th} pixel $y(n)$ in the fused image is obtained as in equation (3) below by linearly combining the pixels $x_k(n)$ at the same location n from the available source images.

$$y(n) = \sum_{k=1}^K w_k(n)x_k(n) = \underline{w}^T(n)\underline{x}(n) \quad (3)$$

Furthermore, we call $\underline{x} = [\underline{x}_1 \ \dots \ \underline{x}_K]^T$ the $K \times NM$ matrix containing all the source images. The same notation is used for the weights, that is to say, $\underline{w} = [w_1 \ \dots \ w_K]^T$.

The weights have to be positive and also $\sum_{i=1}^K w_i(n) = 1$. The aim of the proposed algorithms is to determine the matrix \underline{w} .

3. Dispersion Minimization Fusion (DMF) Based Methods

Recently we introduced a preliminary version of the Dispersion Minimization based Fusion scheme (DMF) [3]. The concept of dispersion was originally studied in its one dimensional form and used for blind equalization of communication signals over dispersive channels [8]. In [3] we investigated the use of two dimensional dispersion to the problem of image fusion [2].

The dispersion constant of a real-valued image F with its zero-mean version denoted by \tilde{F} is defined as follows

$$D_F = \frac{E\{\tilde{F}^4\}}{E\{\tilde{F}^2\}} \quad (4)$$

where $E\{\cdot\}$ denotes the expectation operator performed along the dimension n .

In this work we are seeking for fusion weights that minimize the following cost function

$$J_{CM} = E\{(\tilde{y}^2(n) - D_F)^2\} \quad (5)$$

where D_F is the dispersion value of the original image F defined as in equation (4) above and $\tilde{y}(n)$ denotes the n^{th} pixel of the zero-mean version of the lexicographically ordered fused image \underline{y} . Cost functions similar to that in (5) have been used in communications [8] and the term Constant Modulus (CM) is widely used to refer to them. This term justifies the use of CM as subscript in the notation of the cost function J_{CM} .

It is straightforward from its definition that the cost function in (5) penalizes the deviations of $\tilde{y}^2(n)$ from the dispersion constant D_F . Since a closed form solution for the minimization of (5) does not exist, iterative approaches, as for example the widely used Gradient Descent (GD) method, are

generally used to solve it. The algorithm that performs a stochastic Gradient Descent minimization of a CM type of cost function is referred to in the existing literature as the Constant Modulus Algorithm or CMA [8]. CMA attempts to minimize the CM cost function by starting with arbitrary values for the unknown parameters and following the trajectory of the steepest descent.

In this work, the particularity of the proposed cost function is that we do not know the value of D_F . Therefore, equation (5) involves the estimation of both the fusion weights $[w_1(n), \dots, w_K(n)]$ and the dispersion D_F of the original true scene. Thus, the minimization of (5) is performed using an alternating stochastic Gradient Descent algorithm.

One can notice that in the previous definition we need to deal with zero-mean images. That is why in the rest of the chapter we will use the notation $\tilde{x}(n)$ instead of $x(n)$. However, we will use the non-zero mean version of the source images for the final step, that is to say the reconstruction of the image with the final weights.

From equation (3) we deduct that $\tilde{y}(n) = \underline{w}^T(n)\tilde{x}(n)$ and hence, we can rewrite the proposed cost function as follows.

$$J_{CM}(\underline{w}(n), D_F) = E\{[(\underline{w}^T(n)\tilde{x}(n))^2 - D_F]^2\} \quad (6)$$

In order to minimize the cost function in (6), we are going to use a Gradient Descent method with two learning rates μ and η . We need then to calculate the gradient of $J_{CM}(\underline{w}(n), D_F)$ relative to both $\underline{w}(n)$ and D_F . Throughout the chapter we will often interchange the notations $J_{CM}(\underline{w}(n), D_F)$ and J_{CM} for simplicity.

- **Calculation of $\frac{\partial J_{CM}}{\partial \underline{w}(n)}$**

We know that $J_{CM} = E\{(\tilde{y}^2(n) - D_F)^2\} = E\{\tilde{y}^4(n)\} - 2D_F E\{\tilde{y}^2(n)\} + D_F^2$ and $\tilde{y}(n) = \underline{w}^T(n)\tilde{x}(n)$.

The expectations calculated along the dimension n are approximated by the sample mean

$E\{\tilde{y}^m(n)\} = \frac{1}{MN} \sum_{n=1}^{MN} \tilde{y}^m(n)$. As a result, the derivative of these expectations with respect to the

specific weight $\underline{w}(n)$ will simply be reduced to the derivative of the sample means' term for the corresponding n . Consequently, the requested derivative can be given by

$$\frac{\partial J_{CM}}{\partial \underline{w}(n)} = 4(\tilde{y}^2(n) - D_F)\tilde{y}(n)\tilde{x}(n) \quad (7)$$

- **Calculation of $\frac{\partial J_{CM}}{\partial D_F}$**

From the expression of J_{CM} we have $\frac{\partial J_{CM}}{\partial D_F} = -2 E\{\tilde{y}^2(n)\} + 2 D_F$ or alternatively,

$$\frac{\partial J_{CM}}{\partial D_F} = 2(D_F - E\{\tilde{y}^2(n)\}) \quad (8)$$

3.1 The Dispersion Minimization Fusion method (DMF)

The proposed algorithm is summarized in the steps below.

Initialization

- Set all the weights $\underline{w}(n)$ at the value K^{-1} . The first estimate of the fused image will then be simply the mean of the K source images.
- Set the original value of D_F as the mean of the dispersion parameters of the K source images.

Iteration

- Update the values of $\underline{w}(n)$

$$\underline{w}^+(n) \Leftarrow \underline{w}(n) - \mu \frac{\partial J_{CM}}{\partial \underline{w}(n)}$$

- Normalise the values of $\underline{w}(n)$

$$\underline{w}^+(n) \Leftarrow \text{abs} \left(\frac{\underline{w}(n)}{\|\underline{w}(n)\|} \right)$$

- Update the value of D_F

$$D_F^+ \Leftarrow D_F - \eta \frac{\partial J_{CM}}{\partial D_F}$$

- Check that D_F is positive and if not take its absolute value.

$$D_F^+ \Leftarrow \text{abs}(D_F)$$

The parameters μ and η have a very important role in the convergence of the proposed method. By selecting inappropriate values for these learning rates, the cost function may converge to a local minimum instead of the global minimum. In order to tackle this problem an exhaustive search for optimal combinations of values for μ and η is realized, prior to updating the values for \underline{w} and D_F . By the term optimal we refer to the values that minimize the cost function or yield a value at convergence sufficiently close to the minimum. After a large number of experimental simulations we have concluded that appropriate values for μ lie approximately around 10^{-6} and for η around 0.9. Prior selection of learning rate values enables us to get better results as far as both convergence to the global minimum and speed of convergence are concerned. We shall refer to this modified version of

the method as the Robust DMF method [3]. Once the matrix \underline{w} has converged, the fused image can be reconstructed using the non-zero mean source images.

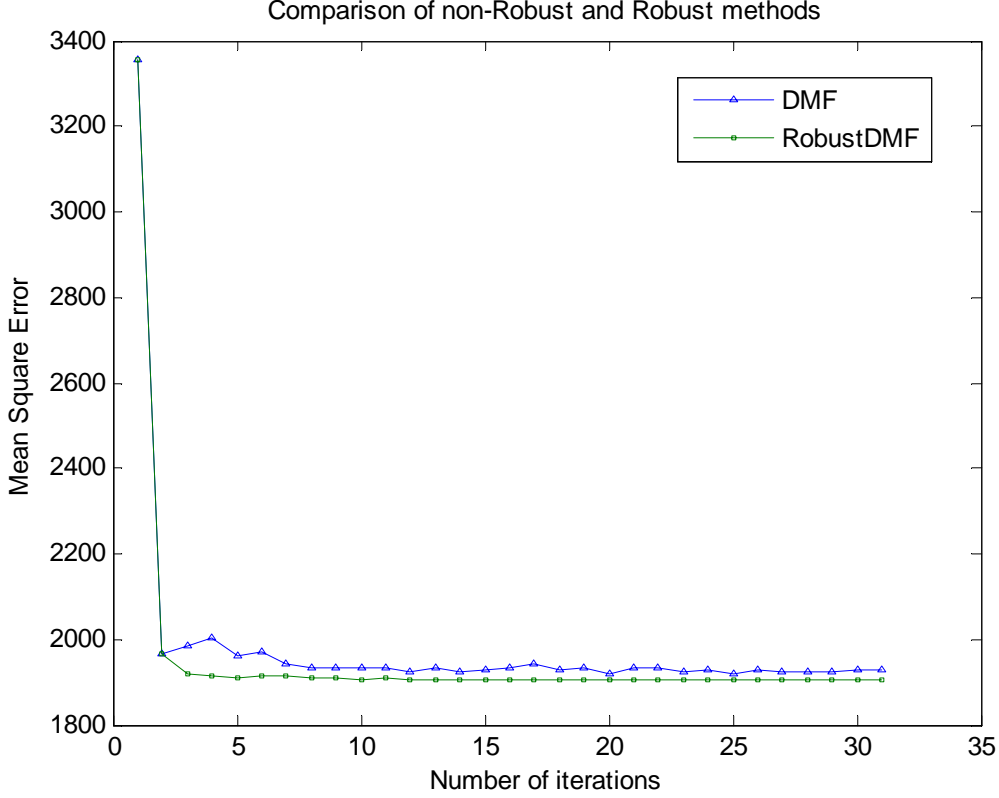


Fig 1: An indicative comparison between DMF and Robust DMF.

3.2 The Dispersion Minimization Fusion method With Neighbourhood (DMF_WN)

In the previous section the update for $\underline{w}(n)$ was essentially estimated using a stochastic update, due to the lack of multiple realisations of the fused image. By assuming that the image signal is locally ergodic we allow the pixels within the $L \times L$ neighbourhood around the pixel of interest n to be treated as multiple realisations of that pixel in the fused image. In addition, we can assume that the weight $\underline{w}(n)$ in this neighbourhood remains constant for each pixel located within the neighbourhood. Consequently, the gradient term can now be calculated via

$$\frac{\partial J_{CM}}{\partial \underline{w}(n)} = E_L \{ 4(\tilde{y}(n)^2 - D_F) \tilde{y}(n) \tilde{\underline{x}}(n) \} \Rightarrow$$

$$\frac{\partial J_{CM}}{\partial \underline{w}(n)} = \begin{bmatrix} E_L \{ 4(\tilde{y}(n)^2 - D_F) \tilde{y}(n) \tilde{x}_1(n) \} \\ \vdots \\ E_L \{ 4(\tilde{y}(n)^2 - D_F) \tilde{y}(n) \tilde{x}_K(n) \} \end{bmatrix} \quad (9)$$

where the expectations $E_L \{ \cdot \}$ are calculated via sample averaging using the pixels located within an

$L \times L$ (L odd) neighbourhood placed symmetrically around pixel n . The optimal size of the neighbourhood depends on the particular image and on the type and severity of distortion. We call this method Dispersion Minimization Fusion method With Neighbourhood (DMF_WN). Regarding the question whether the DMF_WN technique can be combined with the robust version described in Section 3.1, the tests have proved that although it increases the performance it leads to a very long computation time.

4. The Kurtosis Maximization Fusion (KMF) Based Methods

A possible limitation of the previous fusion scheme based on dispersion minimization is that it requires a priori some statistical information, namely, the dispersion value of the ground truth image which is unavailable in practical cases. Although we have formulated a framework of alternating minimization which gives reasonable estimates of the true dispersion value, the instability and bias of the fusion performance could still dominate due to the lack of required information. Therefore, we propose an alternative fusion scheme which is purely based on the available sensor images, and thus, does not require knowledge of the original ground truth image. We refer to this method as Kurtosis Maximization based Fusion scheme (KMF).

The motivation of using kurtosis maximization stems from two facts:

- The Central Limit Theorem states that the probability density function of the sum of several independent random variables tends towards a Gaussian distribution [12].
- Due to the physical limitations of the sensors and imperfect observational conditions, the acquired sensor images represent a degraded version of the original scene by smoothing operators [2] and additive noise [18], which is assumed to be independent to the image scene.

A smoothing operator often acts as a low-pass filter which results in a flatter (more Gaussian) distribution of the filtered image, as the high frequency information is suppressed, degraded or missing [18]. In addition, the combination of an image scene and additive noise, which is independent of the image, further increases the Gaussianity of sensor images due to the Central Limit Theorem. Combining these two facts together, we can see that it is likely that the probability distribution of an image is less Gaussian than that of a distorted version of it or of linear combinations of distorted versions of it [14]. We can assume that the fused image is expected to be as close to the original scene as possible, and furthermore, both the fused image and the original image feature a non-Gaussianity property. Such a principle implies that if we find a fused image Y that follows the minimum Gaussian behaviour (or alternatively, maximum non-Gaussianity), then that image will be closer to the original scene F compared to the acquired sensor images. To some extent, non-Gaussianity reflects the quality of the fused image. We can therefore identify the optimal fused image by maximizing its non-Gaussianity via updating the fusion weights. To quantify the non-Gaussianity of

the image, measurements, such as high order central moments are frequently used. Here we choose the absolute value of kurtosis, a normalized fourth order central moment, to serve for non-Gaussianity maximization.

Consider an image F . We define the kurtosis K_F of its zero-mean version \tilde{F} as

$$K_F = \frac{\text{cum}_4\{\tilde{F}\}}{E^2\{\tilde{F}^2\}} = \frac{E\{\tilde{F}^4\} - 3E^2\{\tilde{F}^2\}}{E^2\{\tilde{F}^2\}} = \frac{E\{\tilde{F}^4\}}{E\{\tilde{F}^2\}E\{\tilde{F}^2\}} - 3 = \frac{D_F}{\sigma_{\tilde{F}}^2} - 3 \quad (10)$$

where $\text{cum}_4\{\tilde{F}\}$ and $\sigma_{\tilde{F}}^2$ denote the fourth order cumulant and the standard deviation of \tilde{F} , respectively. From a statistical perspective, kurtosis measures the peakedness of a distribution [9]. More specifically, a Gaussian distribution has kurtosis equal to zero ($K_F = 0$). Moreover, it exhibits moderate tails and it is called mesokurtic. A distribution with small tails has negative kurtosis ($K_F < 0$) and is called sub-Gaussian or platykurtic and one with long tails has positive kurtosis ($K_F > 0$) and is called super-Gaussian or leptokurtic. The absolute value of kurtosis is usually used as a measurement of non-Gaussianity as it tends to be zero for a Gaussian distribution and non-zero for any other non-Gaussian distribution. In order to demonstrate the correlation among distortion, non-Gaussianity and the absolute value of kurtosis, we assume the original image Cameraman and a distorted version of it by Gaussian blur. The histograms and the absolute kurtosis of the two images are illustrated in Fig. 2 below, in which we observe that when distortion occurs, the corresponding $|K_F|$ value decreases as the image data becomes more Gaussian. In other words, it is safe to state that the actual non-distorted representation of the observed scene, and therefore the fused image that is produced using the available sources have larger values of $|K_F|$, or alternatively follow a more non-Gaussian behaviour and are less distorted. Inspired by the fact that the absolute value of $|K_F|$ (non-Gaussianity) can be a sound criterion to reflect the quality of a fused image, we derive a novel fusion scheme, which solves for optimal fusion weights by maximizing a non quadratic cost function J_K , describing the absolute value of the kurtosis of the fused image Y .

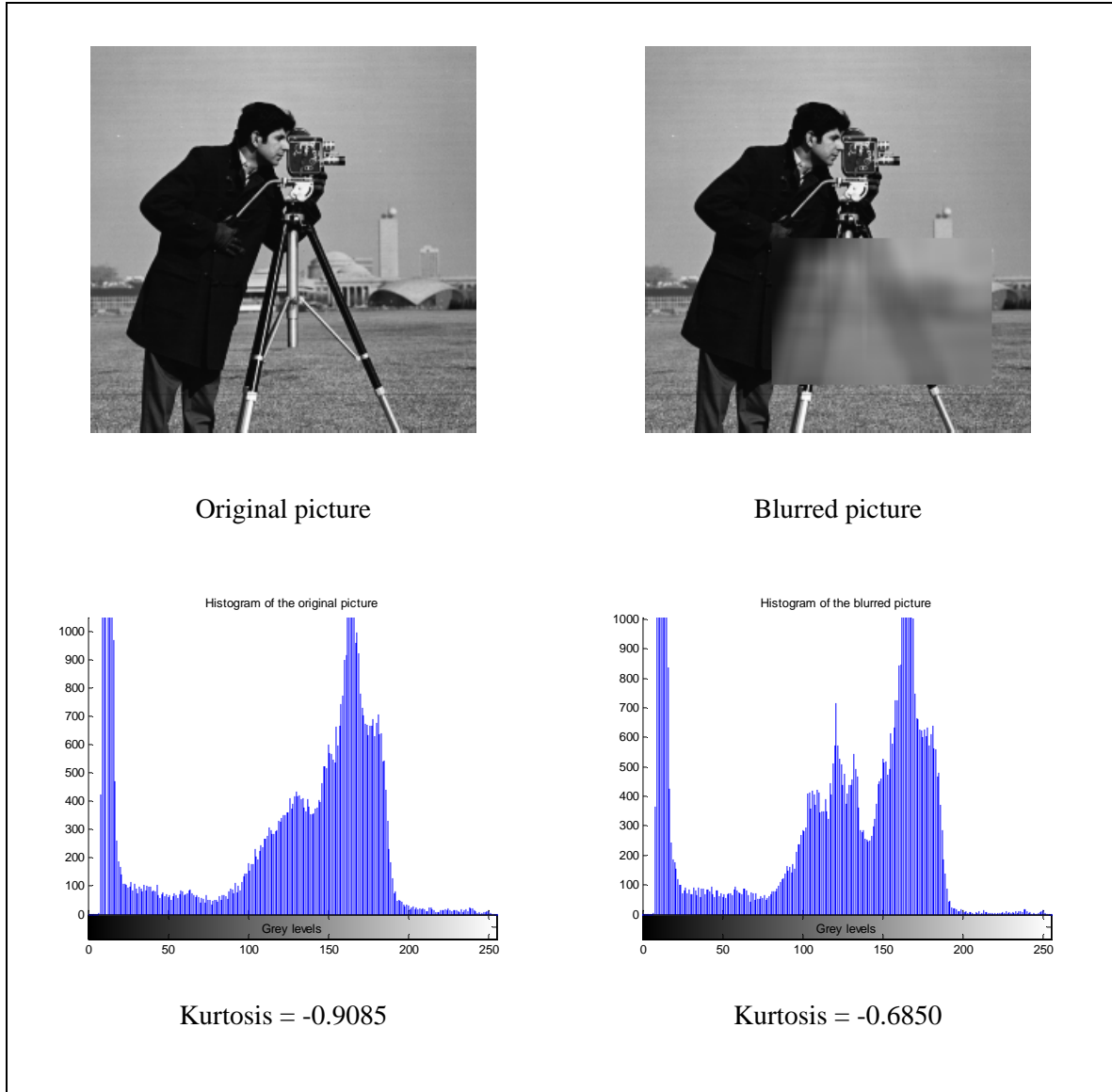


Fig 2: Histograms and kurtosis of two pictures

Based on the above analysis, it seems logical to choose for the cost function the absolute value of the kurtosis

$$J_K = |K_F| = \left| \frac{E\{\tilde{y}^4(n)\}}{E^2\{\tilde{y}^2(n)\}} - 3 \right| \quad (11)$$

where $\tilde{y}(n)$ denotes the n^{th} pixel of the zero-mean version of the lexicographically ordered fused image \underline{y} as already mentioned. Using equation (3) we can rewrite the cost function as follows.

$$J_K(w(n)) = \left| \frac{E\{(w^T(n)\tilde{x}(n))^4\}}{E^2\{(w^T(n)\tilde{x}(n))^2\}} - 3 \right| \quad (12)$$

We therefore need to maximize a cost function depending on one unknown parameter, namely, the

vector $\underline{w}(n)$. To solve this problem we will again use a Gradient Descent method with one learning rate λ . We need then to calculate the gradient of $J_K(\underline{w}(n))$ relative to $\underline{w}(n)$. Throughout the chapter we will often interchange the notations $J_K(\underline{w}(n))$ and J_K for simplicity.

- **Calculation of $\frac{\partial J_K}{\partial \underline{w}(n)}$**

$$J_K = \frac{|E\{\tilde{y}^4(n)\} - 3E^2\{\tilde{y}^2(n)\}|}{E^2\{\tilde{y}^2(n)\}} = \frac{|\text{cum}_4\{\tilde{y}(n)\}|}{E^2\{\tilde{y}^2(n)\}}$$

$$\frac{\partial J_K}{\partial \underline{w}(n)} = \frac{1}{E^4\{\tilde{y}^2(n)\}} \left[\frac{\partial |\text{cum}_4\{\tilde{y}(n)\}|}{\partial \underline{w}(n)} E^2\{\tilde{y}^2(n)\} - \frac{\partial E^2\{\tilde{y}^2(n)\}}{\partial \underline{w}(n)} |\text{cum}_4\{\tilde{y}(n)\}| \right]$$

$$\text{where } \frac{\partial E^2\{\tilde{y}^2(n)\}}{\partial \underline{w}(n)} = 2E\{\tilde{y}^2(n)\} \frac{\partial E\{\tilde{y}^2(n)\}}{\partial \underline{w}(n)} = 4E\{\tilde{y}^2(n)\}E\{\tilde{y}(n)\tilde{x}(n)\}$$

$$\text{and } \frac{\partial |\text{cum}_4\{\tilde{y}(n)\}|}{\partial \underline{w}(n)} = \text{sgn}(\text{cum}_4\{\tilde{y}(n)\}) \left[\frac{\partial E\{\tilde{y}^4(n)\}}{\partial \underline{w}(n)} - 3 \frac{\partial E^2\{\tilde{y}^2(n)\}}{\partial \underline{w}(n)} \right] \Rightarrow$$

$$= 4 \text{sgn}(\text{cum}_4\{\tilde{y}(n)\}) \left[E\{\tilde{y}^3(n)\tilde{x}(n)\} - 3E\{\tilde{y}^2(n)\}E\{\tilde{y}(n)\tilde{x}(n)\} \right]$$

and hence,

$$\begin{aligned} \frac{\partial J_K}{\partial \underline{w}(n)} &= \\ & 4 \frac{\text{sgn}(\text{cum}_4\{\tilde{y}(n)\})}{E^4\{\tilde{y}^2(n)\}} [E^2\{\tilde{y}^2(n)\}E\{\tilde{y}^3(n)\tilde{x}(n)\} - 3E^3\{\tilde{y}^2(n)\}E\{\tilde{y}(n)\tilde{x}(n)\} - E\{\tilde{y}^2(n)\}E\{\tilde{y}(n)\tilde{x}(n)\}\text{cum}_4\{\tilde{y}\}] \\ &= 4 \frac{\text{sgn}(\text{cum}_4\{\tilde{y}(n)\})}{E^3\{\tilde{y}^2(n)\}} [E\{\tilde{y}^2(n)\}E\{\tilde{y}^3(n)\tilde{x}(n)\} - E\{\tilde{y}^4(n)\}E\{\tilde{y}(n)\tilde{x}(n)\}] \end{aligned}$$

As in the dispersion case, the expectation $E\{\cdot\}$ is referring to multiple realisations of the fused image. If we assume that there is only a single realisation, i.e., the image $\tilde{y}(n)$, then the expectation can be dropped for a stochastic update of the gradient. Equally, we can assume that an $L \times L$ neighbourhood around pixel n contains pixels that can serve as multiple realisations of $\tilde{y}(n)$ if local ergodicity exists. In this case, the expectations can be estimated by sample averaging using the pixels in this neighbourhood, assuming a single weight vector $\underline{w}(n)$ for all these pixels.

4.1 The Kurtosis Minimization Fusion method (KMF)

The proposed algorithm is summarized in the steps below.

Initialization

- Set all the weights at the value K^{-1} . The first iteration of the fused image will then be simply the mean of the K source images.

Iteration

- Update the values of $\underline{w}(n)$

$$\underline{w}^+(n) \leftarrow \underline{w}(n) - \lambda \frac{\partial J_K}{\partial \underline{w}(n)}$$

- Normalise the values of $\underline{w}(n)$

$$\underline{w}^+(n) \leftarrow \text{abs} \left(\frac{\underline{w}(n)}{\|\underline{w}(n)\|} \right)$$

Once the matrix \underline{w} has converged, the fused image can be reconstructed using the non-zero mean source images.

4.2 The Robust Kurtosis Minimization Fusion method (Robust KMF)

As with the DMF method we can also use here an optimized learning rate λ . An exhaustive search for optimal values for λ is realized, prior to updating the values of \underline{w} . We shall refer to this modified version of the method as the Robust KMF method.

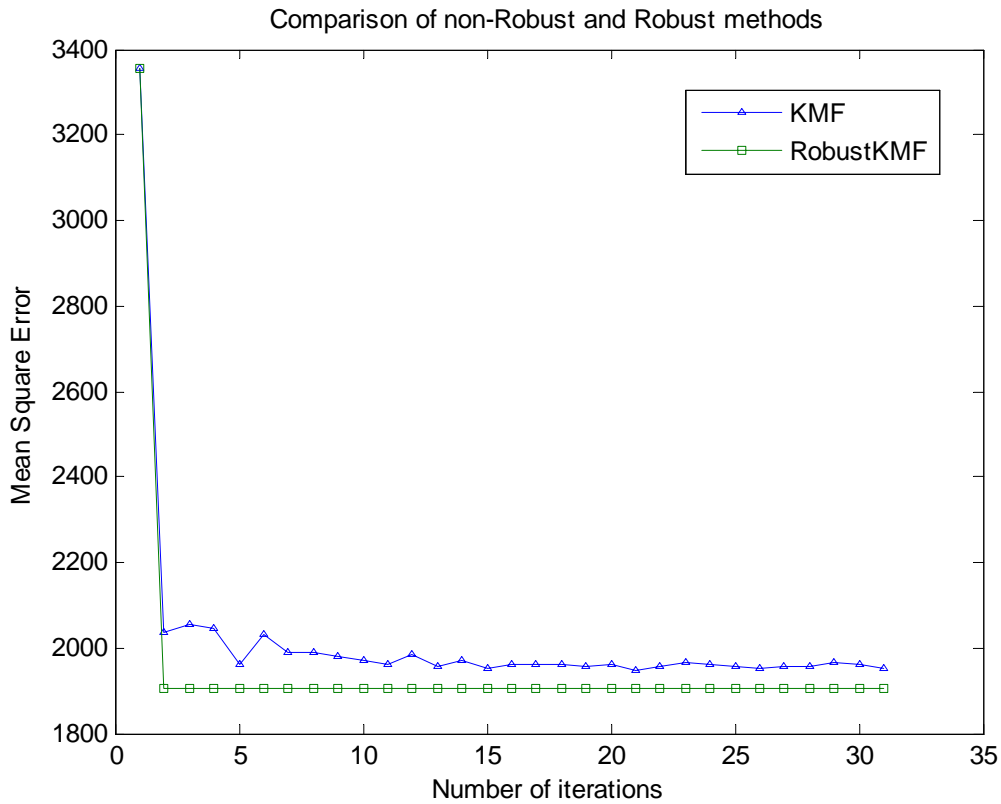


Fig 3: An indicative comparison between KMF and Robust KMF.

5. Experimental Results

In order to evaluate the performance of the proposed methods we will compare them to the following well known methods on a selection of sets of images.

- Dual-Tree Wavelet Transform (**DT_WT**). This is a widely used transform domain method based on wavelet transforms. We use for evaluation this method in conjunction with the so called max-abs fusion rule. One can find further analysis in [7].
- Error Estimation Fusion (**EEF**). This is a spatial domain iterative method which has been developed very recently and uses the so called robust error estimation theory [5].

In order to provide numerical results we will use the following image fusion performance metrics.

- Q_0 stands for the so called Universal Image Quality Index. This is a measurement that evaluates the quality of an image in general and requires the ground truth in order to be calculated [11].
- MG stands for mean gradient image quality assessment method [10].
- S stands for the Petrovic image fusion metric [12].
- Q , Q_W , Q_e stand for the three variations of the Piella image fusion metric [6].

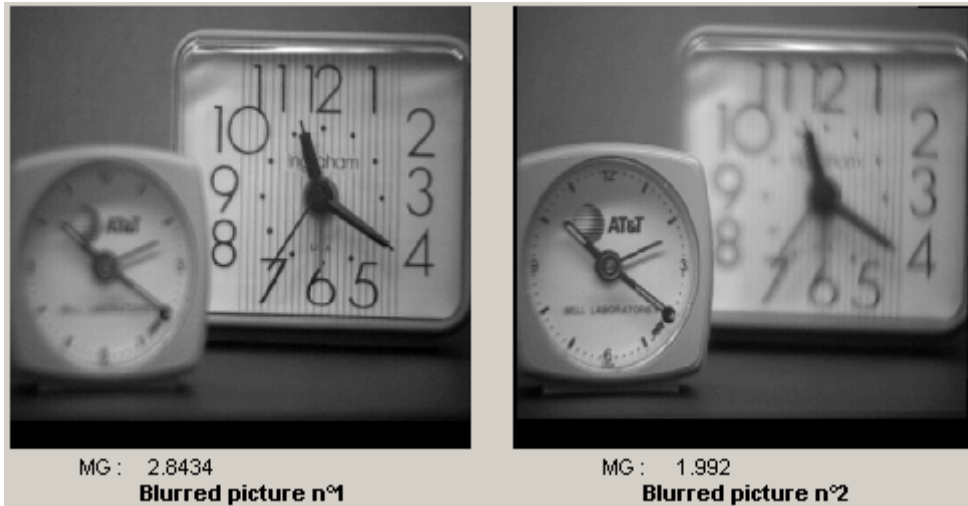
When we have the choice of robust and non robust version of a method we will always choose the robust version since it always exhibits improved performance. In these cases as well as in the EEF method 15 iterations approximately are often enough. In the DMF_WN we realize 10 iterations since the computation time is often very long. Therefore, for each set of images we will apply the following techniques.

- Robust KMF
- Robust DMF
- DMF_WN, small neighbourhood 3×3
- DMF_WN, large neighbourhood 9×9 or 15×15
- DT_WT, max-abs fusion rule
- EEF

What follows is a description of the experiments.

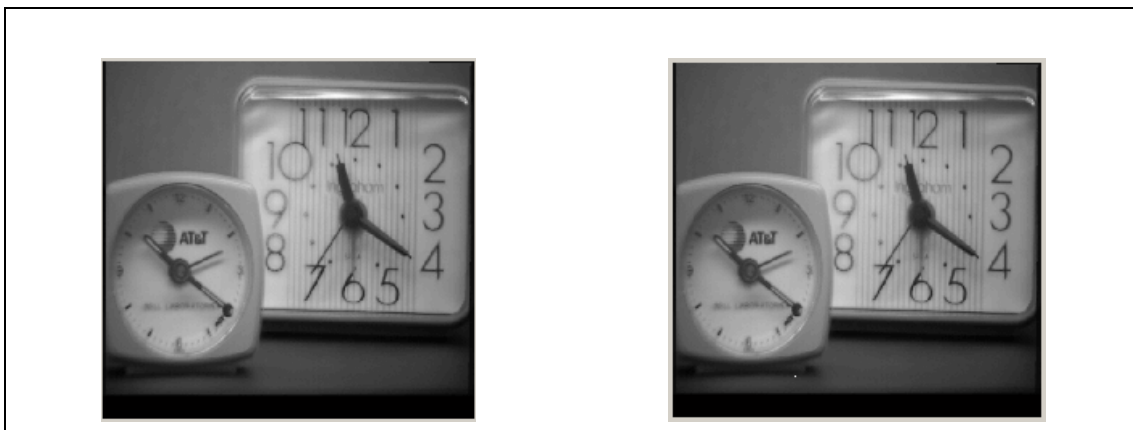
5.1 Case one : Multi-focus images, small amount of distortion

Example 1: Clocks



As shown in the Table below the results obtained using the proposed techniques are not very encouraging compared to the DT_WT method in the context of the image fusion metrics used. The edges of the big clock still remain quite blurred. However, the DMF_WN with a large neighbourhood (9×9) yields acceptable results. Considering that the input images are large (512×512), this is the largest size of local neighbourhood we can take without facing serious computational burden. The numbers shown in bold demonstrate the best performance achieved among the various methods in terms of the corresponding metric.

	Robust KMF	Robust DMF	DMF_WN 3×3	DMF_WN 9×9	DT_WT	EEF
Q	0.8259	0.8258	0.8298	0.8408	0.7387	0.8404
Q_w	0.8554	0.8553	0.8492	0.8835	0.9120	0.8761
Q_e	0.5839	0.5843	0.5846	0.6676	0.8092	0.6552
S	0.58606	0.58627	0.59304	0.62443	0.67478	0.6356
MG	2.328	2.3236	2.3039	2.2832	3.4056	2.2302



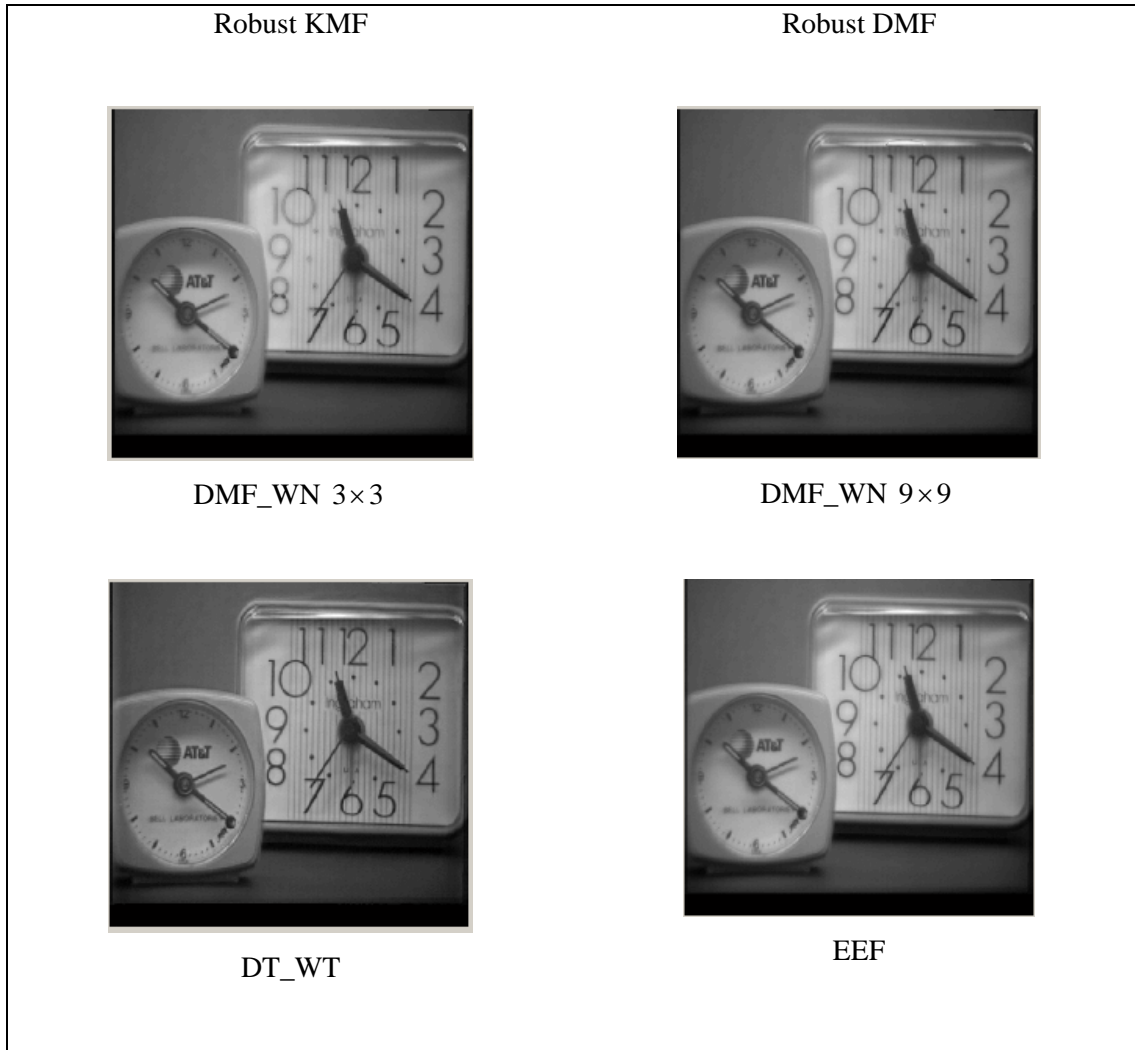
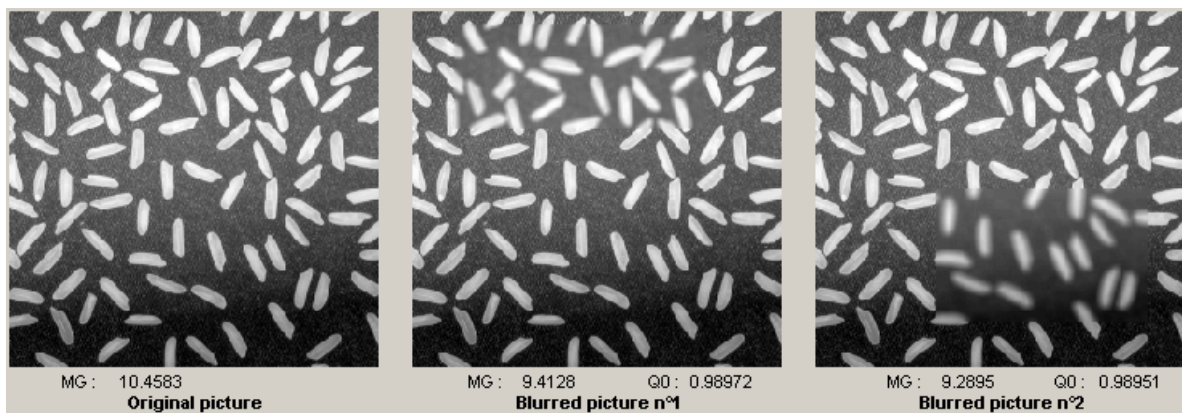


Fig 4: The “Clocks’ example

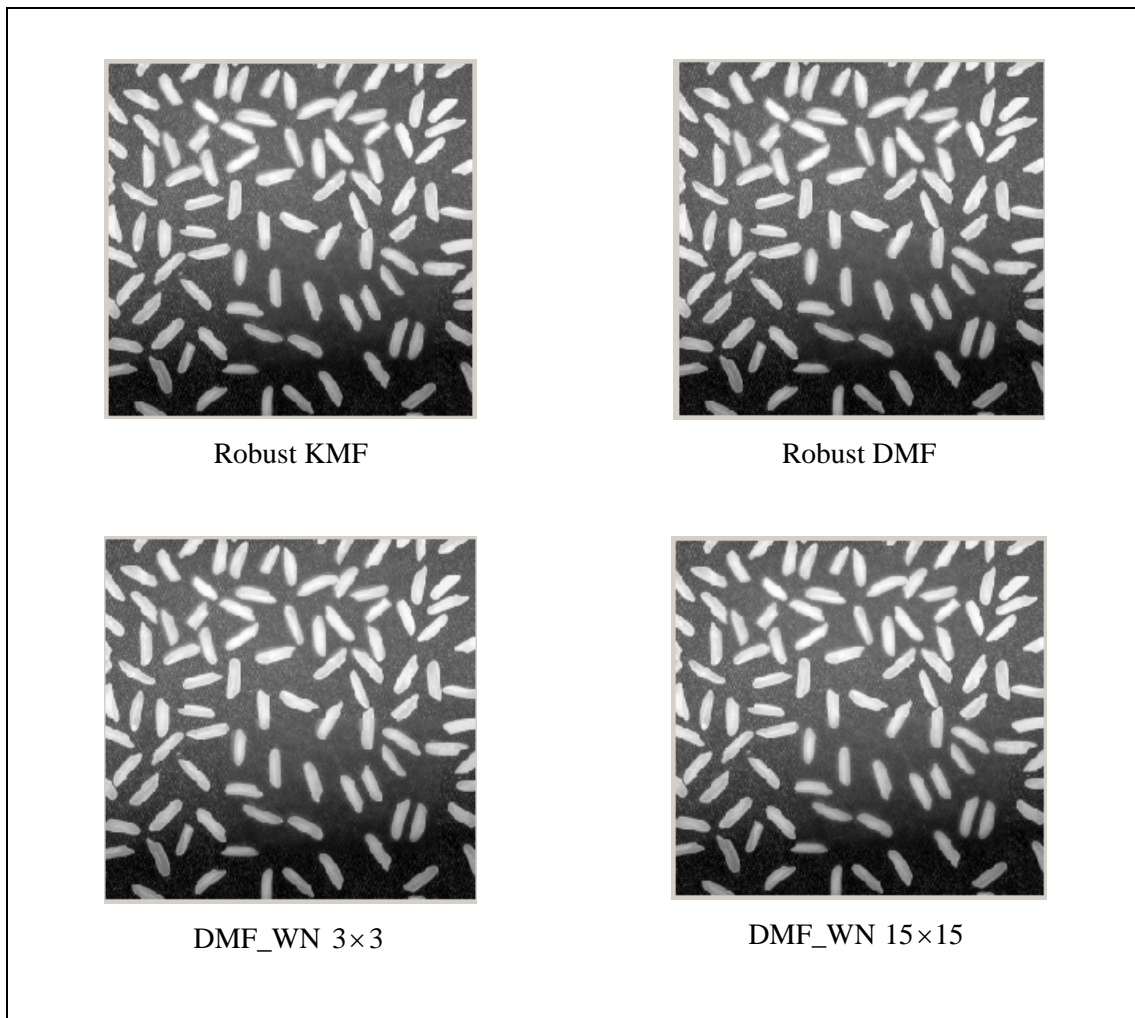
Example 2: Rice



We applied a small amount of blur on the ‘rice’ image. While the DT_WT method works very well, the proposed methods aren’t visually very efficient. We see that the fused image remains blurred and

the result is not very detailed. However, the metrics exhibit good values for the four proposed methods. This observation establishes the universally accepted rule that image fusion metrics do not always reflect the visual quality of an image.

	Robust KMF	Robust DMF	DMF_WN 3×3	DMF_WN 15×15	DT_WT	EEF
Q_0	0.995	0.99491	0.99616	0.99562	0.99901	0.99643
Q	0.9440	0.9433	0.9522	0.9524	0.9520	0.9498
Q_w	0.9757	0.9754	0.9786	0.9792	0.9734	0.9792
Q_e	0.9110	0.9102	0.9246	0.9198	0.9338	0.9262
S	0.8768	0.87583	0.88626	0.88988	0.86172	0.88272
MG	9.294	9.3048	9.278	9.1277	10.5312	9.1099



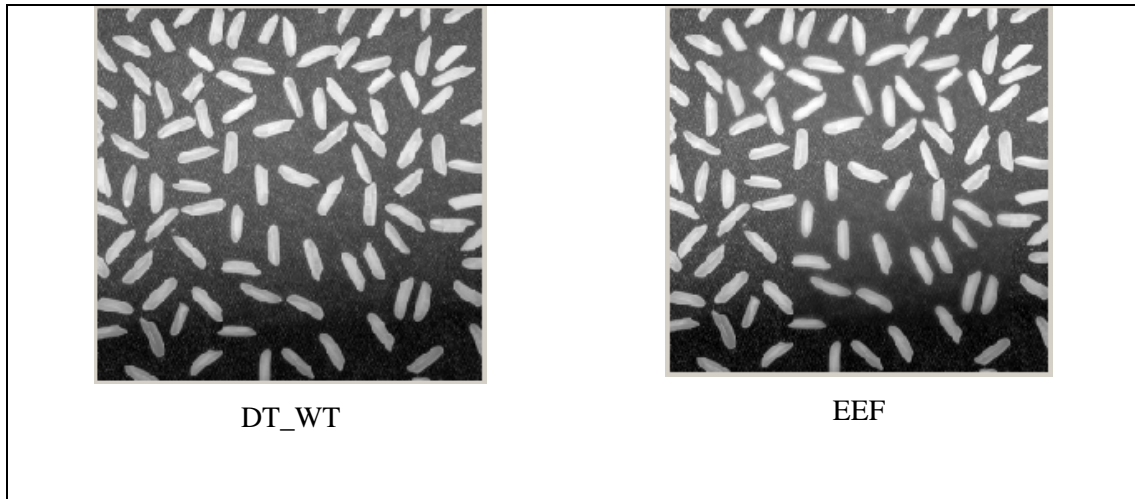


Fig 5: The 'Rice' Example

5.2 Case two : Multi-focus images, severe distortion

Example 1: Cameraman



In this example we applied severe distortion on the 'cameraman' image. The proposed methods exhibit now a distinctively improved performance. The Robust DMF and Robust KMF methods are superior compared to the spatial domain EEF method in terms of the image fusion metrics used. Regarding the DMF_WN method with large sizes of local neighbourhood, it possibly exhibits the best performance, even better than the widely accepted DT_WT. It appears from a large number of experiments that the proposed methods are very efficient in the case of severe distortion. The DT_WT tends to create some discontinuities in the image while the Robust DMF and Robust KMF provide really good visual results. Our methods are in this example the only ones where the original areas of distortion are not visible.

	Robust KMF	Robust DMF	DMF_WN 3×3	DMF_WN 15×15	DT_WT	EEF
Q_0	0.99265	0.99261	0.99334	0.99605	0.99455	0.98919
Q	0.8948	0.8948	0.8963	0.9062	0.8729	0.9040
Q_w	0.9509	0.9506	0.9542	0.9672	0.9681	0.9491
Q_e	0.8901	0.8892	0.9031	0.9302	0.9487	0.9022
S	0.87097	0.87019	0.8734	0.89113	0.88752	0.86997
MG	8.8364	8.8375	9.0073	9.0431	10.1157	8.8082



Robust KMF



Robust DMF



DMF_WN 3×3

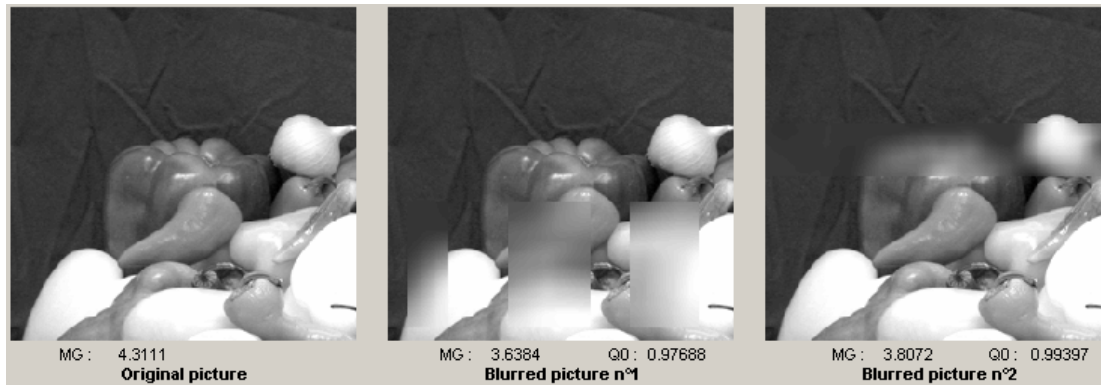


DMF_WN 15×15



Fig 6: The 'Cameraman' example

Example 2: Peppers



Severe blur is also applied to various areas of the 'peppers' image. In the DT_WT method the distorted areas are still visible. However, in our methods it is harder to visualize where the original distortion was. Therefore, we can claim that in this example our methods give better results.

	Robust KMF	Robust DMF	DMF_WN 3×3	DMF_WN 15×15	DT_WT	EEF
Q_0	0.99421	0.99435	0.99446	0.99551	0.99497	0.9941
Q	0.8964	0.8970	0.8971	0.9100	0.8549	0.9140
Q_w	0.8969	0.8981	0.8998	0.9210	0.9462	0.9292
Q_e	0.7495	0.7538	0.7651	0.8063	0.9009	0.8402
S	0.80689	0.80947	0.81066	0.82009	0.82661	0.82606
MG	3.7699	3.7244	3.7378	3.6913	4.5186	3.7229



Fig 7: The 'Peppers' example

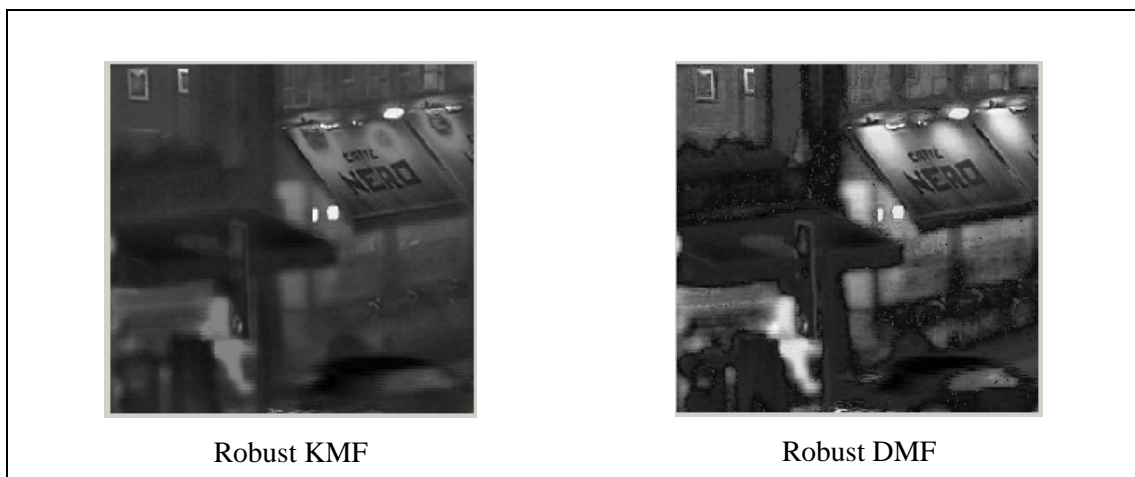
5.3 Case three : Multi-sensor images

Example 1: Infra Red / Dark photo



One can notice that in this example the Robust DMF fused image is the sharpest, even if some “salt and pepper” noise artefacts seem to appear. The Robust KMF is nevertheless the clearest. Depending on what one expects from the fusion these two methods give very good results. It is interesting to observe that the DMF_WN method which gave us good results previously fails here. However, in terms of metric the DT_WT seems to perform better.

	Robust KMF	Robust DMF	DMF_WN 3×3	DMF_WN 15×15	DT_WT	EEF
Q	0.5537	0.3650	0.3761	0.4631	0.6809	0.5718
Q_w	0.6673	0.7055	0.7204	0.7921	0.8402	0.7680
Q_e	0.4184	0.4824	0.5375	0.6167	0.7796	0.6459
S	0.39238	0.41474	0.44032	0.49446	0.60084	0.48381
MG	3.6275	7.6672	7.2204	5.9965	6.7304	4.4191



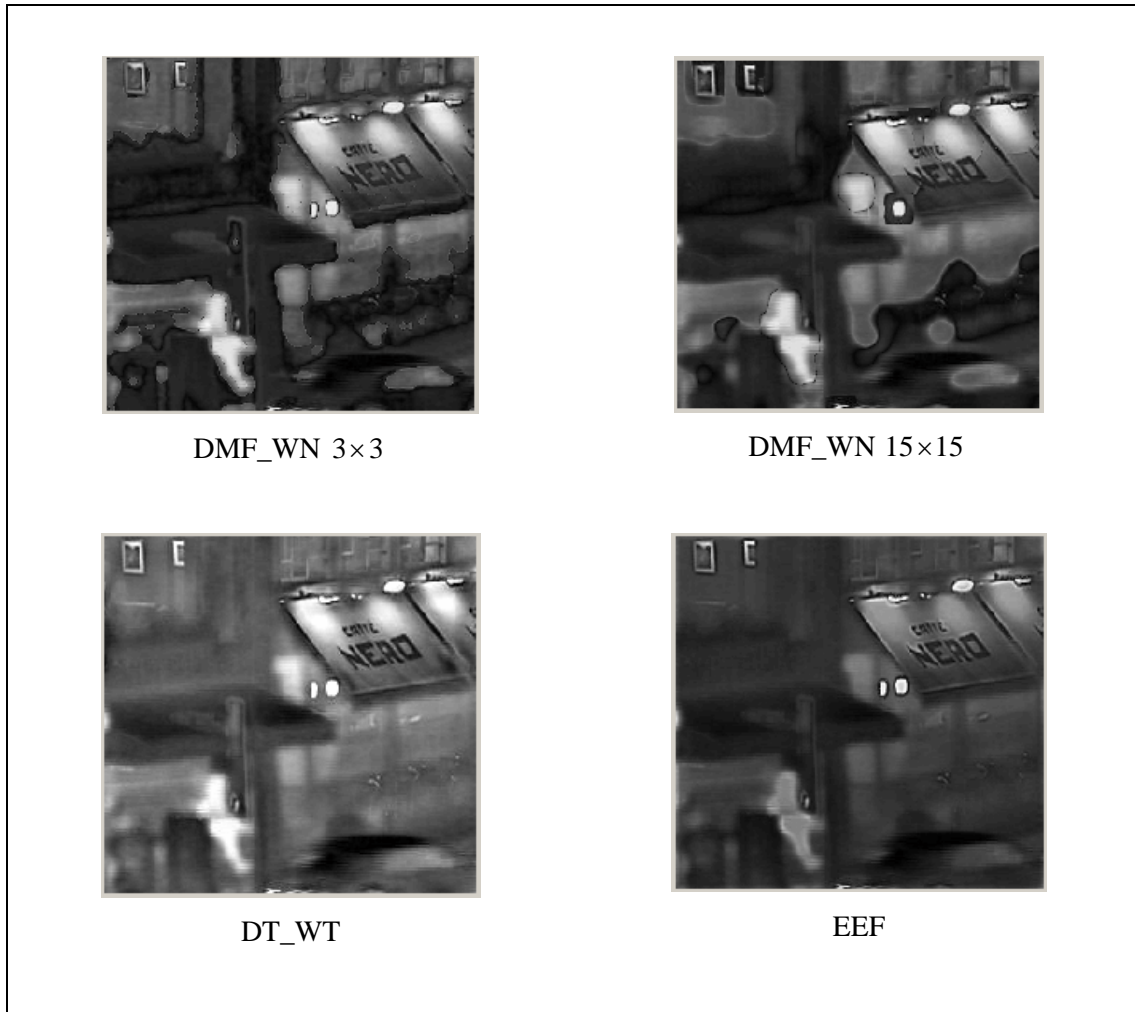
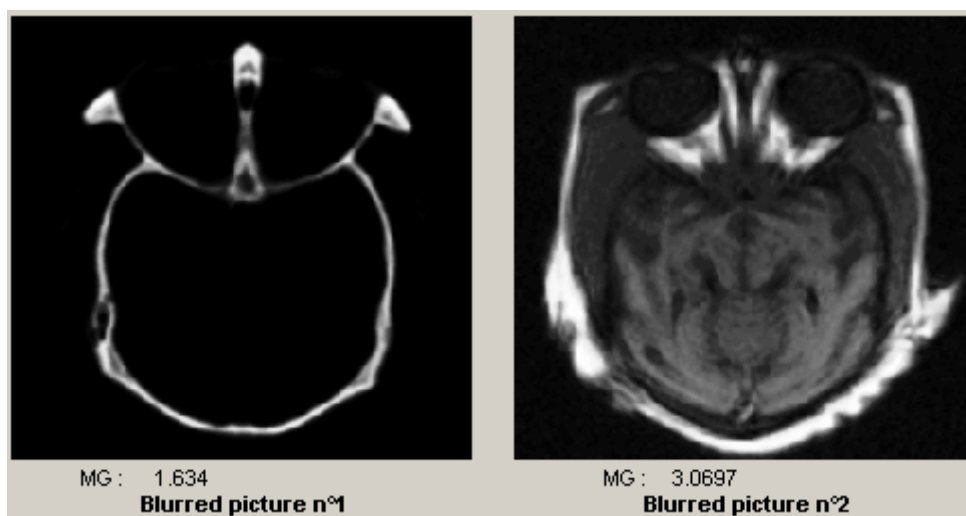


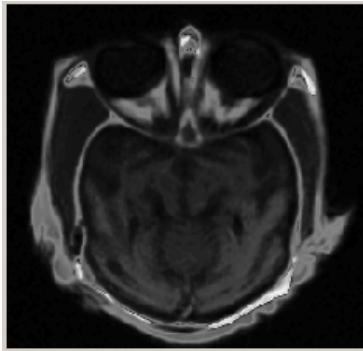
Fig 8: The 'Coffee Shop' example

Example 2: Medical photos

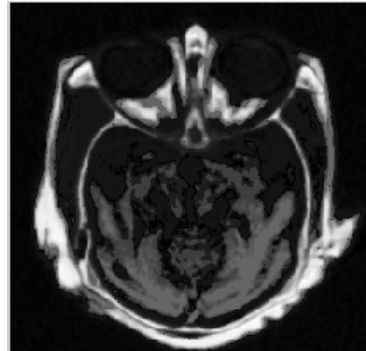


The Robust DMF and KMF provide good visual results although the corresponding metrics are not again the best. One can notice that the DMF_WN with 15×15 neighbourhood provides the best Universal Image Quality Index but there are blocking artefacts present in the fused image which are visually irritating.

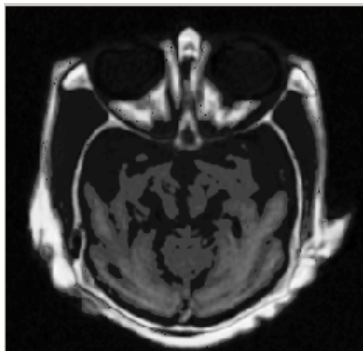
	Robust KMF	Robust DMF	DMF_WN 3×3	DMF_WN 15×15	DT_WT	EEF
Q	0.6451	0.7114	0.8138	0.8085	0.7939	0.6499
Q_w	0.6417	0.7997	0.8231	0.7394	0.8301	0.7042
Q_e	0.3618	0.5632	0.6271	0.5086	0.6605	0.4818
S	0.51682	0.63921	0.7067	0.6442	0.70103	0.55065
MG	2.5105	4.1956	3.8514	3.5105	4.2258	2.4108



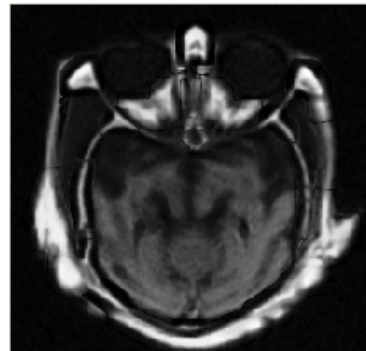
Robust KMF



Robust DMF



DMF_WN 3×3



DMF_WN 15×15

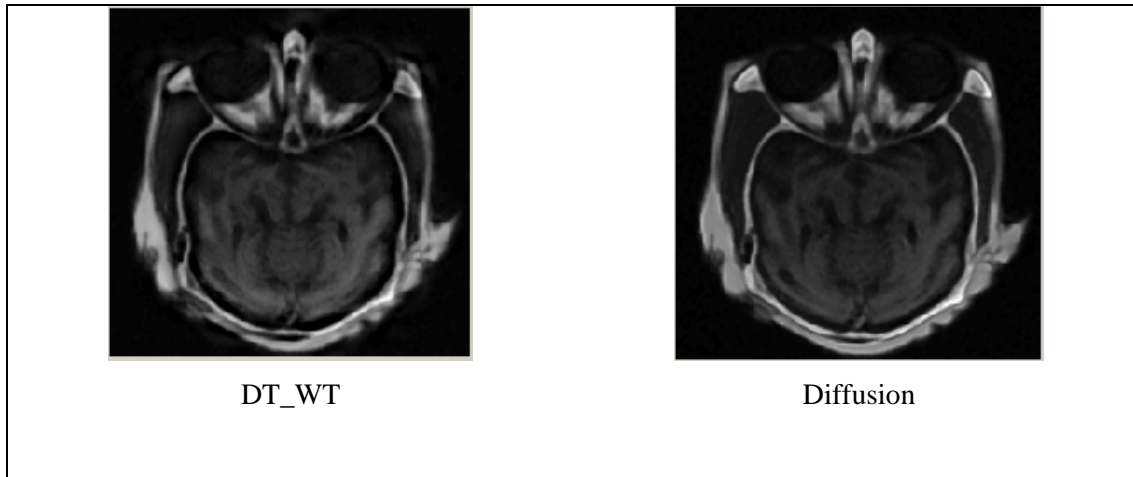


Fig 9: The ‘Medical’ example

6. Conclusions

Throughout this chapter we have described new spatial domain methods for multi-focus and multi-sensor image fusion. The mathematical background relevant to the proposed techniques is based on the iterative solution of two novel optimization formulations related to the statistical properties of the original unknown image. In the experimental results presented in this chapter, it is highlighted that the proposed methods provide good results in almost every situation in terms of the widely used image fusion performance evaluation metrics. The only scenario where the proposed methods seem to be weak is the multi-focus scenario where the source images exhibit light distortion. Moreover, the visual assessment of the proposed methods is encouraging, although it is important to stress out the fact that the evaluation of image fusion results depends on the perception of the individual viewer. The introduction of the robust version of the proposed methods does not enhance visually the fusion results but enables us to obtain good results with less number of iterations. The local neighbourhood method yields better results although the optimal size of the neighbourhood is still a parameter under investigation and depends on the particular image set scenario. Among the proposed methods, for multi-focus image scenarios one will rather choose the DMF_WN or the Robust KMF method, while for multi-sensor image scenarios the Robust DMF or the Robust KMF would be more appropriate.

References

- [1] John, S., Vorontsov, M. “Multi-frame Selective Information Fusion from Robust Error Estimation Theory”, *IEEE Transactions on Image Processing*, Volume 14, Issue 5, May 2005 Page(s): 577 – 584.

- [2] Li, D.L., Mersereau, R.M., and Simske, S., “Blur Identification Based on Kurtosis Minimization”, *Proceeding of the IEEE International Conference on Image Processing*, Volume: 1, Sept. 2005, Page(s): I- 905-8.
- [3] Li, Q., Stathaki, T., “Image Fusion Using Dispersion Minimisation”, *Proceeding of IEEE International Conference on Acoustic, Sound and Signal Processing*, Toulouse, France, 2006
- [4] Mitianoudis N., Stathaki T., “Pixel-Based and Region-Based Image Fusion Schemes Using ICA Bases”, *Elsevier Journal of Information Fusion*, 8 (2), pp. 131–142, April 2007.
- [5] Mitianoudis N., Stathaki T., “Joint Fusion and Blind Restoration for Multiple Image Scenarios with Missing Data”, to appear in *The Computer Journal*.
- [6] Piella G., Heijmans, H., “A New Quality Metric for Image Fusion”, *Proceedings of the IEEE International conference on Image Processings*, Volume 3, Sept. 2003, Page(s): III - 173-6.
- [7] Selesnick I.W., Baraniuk, R.G., Kingsbury N.G., “The Dual-Tree Complex Wavelet Transform”, *IEEE Signal Processing Magazine*, Volume 22, Issue 6, Nov. 2005, Page(s): 123 – 151.
- [8] Treichler, J.R. and Agee, B.G., “A New Approach to Multipath Correction of Constant Modulus Signals”, *IEEE Transactions on Acoustics, Speech and Signal Processing*, Volume 31, Issue 2, Apr 1983 Page(s): 459 – 472.
- [9] Yang, J., Blum, R.S., A Statistical Signal Processing Approach to Image Fusion using Hidden Markov Models for the book *Multi-Sensor Image Fusion and Its Applications*, Marcel Dekker/CRC, 2005. Editors: R. Blum and Z. Liu.
- [10] Wald, L., Ranchin, T., Mangolini, M., “Fusion of Satellite Images of Different Spatial Resolution : Assessing the Quality of Resulting Images”, *Photogrammetric Engineering and Remote Sensing*, Volume 63, No. 6, pp. 691-699, 1997.
- [11] Wang, Z. and Bovik, A.C., “A Universal Image Quality Index”, *IEEE Signal Processing Letters*, Volume 9, Issue 3, Mar 2002, Page(s): 81 – 84.
- [12] Xydeas, C.S., Petrovic, V., “Objective Image Fusion Performance Measure”, *Electronics Letters*, Volume 36, Issue 4, 17 Feb 2000 Page(s):308 – 309.